10.2478/acsc-2014-0018

Archives of Control Sciences
Volume 24(LX), 2014
No. 3, *pages 299–319*

Iterative learning control with sampled-data feedback for robot manipulators

KAMEN DELCHEV, GEORGE BOIADJIEV, HARUHISA KAWASAKI and TETSUYA MOURI

This paper deals with the improvement of the stability of sampled-data (SD) feedback control for nonlinear multiple-input multiple-output time varying systems, such as robotic manipulators, by incorporating an off-line model based nonlinear iterative learning controller. The proposed scheme of nonlinear iterative learning control (NILC) with SD feedback is applicable to a large class of robots because the sampled-data feedback is required for model based feedback controllers, especially for robotic manipulators with complicated dynamics (6 or 7 DOF, or more), while the feedforward control from the off-line iterative learning controller should be assumed as a continuous one. The robustness and convergence of the proposed NILC law with SD feedback is proven, and the derived sufficient condition for convergence is the same as the condition for a NILC with a continuous feedback control input. With respect to the presented NILC algorithm applied to a virtual PUMA 560 robot, simulation results are presented in order to verify convergence and applicability of the proposed learning controller with SD feedback controller attached.

Key words: sampled-data systems, iterative learning control, robot manipulators, convergence analysis

1. Introduction

Sampled-data systems are a class of control systems, where a continuous-time plant is controlled by a discrete-time controller [1-3]. The stabilization of sampled-data systems (SD stabilization problem) is motivated by the use of digital computers in most recent controllers. In particular, a robot arm with rotational joints controlled by a programmable industrial controller is a typical nonlinear time-varying sampled-data (SD) system. The difference between the discrete system and the SD one is shown in Fig. 1(a) and Fig. 1(b), correspondingly, where $\boldsymbol{P}$ is a plant and $\boldsymbol{C}$ is a feedback controller, solid

K. Delchev is with Institute of Mechanics, Bulgarian Academy of Sciences, "Acad.G.Bonchev" Str., bl.4, BG-1113 Sofia. E-mail: kamen@imbm.bas.bg. G. Boiadjiev is with Faculty of Mathematics and Informatics, Sofia University, 1164 Sofia, 5 James Bourchier Blvd., Bulgaria. H. Kawasaki and T. Mouri are with Department of Human and Information Systems, Gifu University, 1-1 Yanagido, Gifu, 501-1193, Japan.

The support by the project No. 079/08.05.2014 "Robot system application for the accuracy increasing during bone drilling in the orthopaedic surgery", granted by Science Research Funding of Sofia University, is acknowledged.

Received 31.07.2014.

lines represent continuous signals and dotted lines represent discrete signals, and $\boldsymbol{S}$ and $\boldsymbol{H}$ are a sampler (Analog to Digital Converter) and a holder (Digital to Analog Converter), correspondingly, and $t \in [0,T]$, $\{t_k : t_k = kt^s\}_{k=0}^{K} \subset [0,T]$, $K = \lfloor T/t^s \rfloor$, where $\lfloor\rfloor$ denotes the integer part of a real number, and t^s is the sampling interval. Three basic approaches for SD controller design are discussed by Petrew et al. [1]: 1) continuous-time emulation design, 2) discrete-time discretization design, and 3) sampled-data direct design. Unfortunately, the efficiency of these methods for SD system stabilization requires sufficiently high sampling rate. Therefore, in [4] a feedforward gain was proposed to improve significantly control efficiency. It is well known in the literature [5-7] that the best approach for an improvement of the feedforward control for uncertain systems is the Iterative Learning Control (ILC).

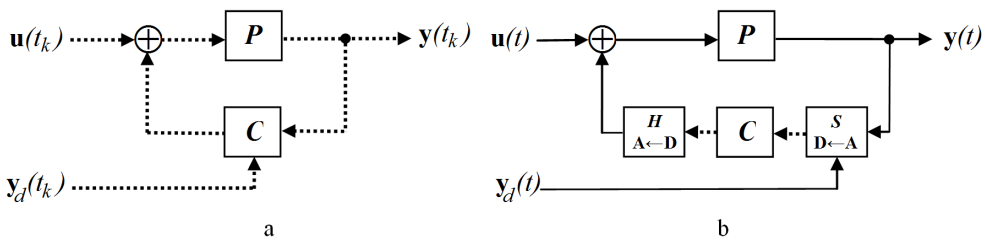

Figure 1. (a) Control of a discrete system [1]; (b) Control of a sampled-data system [1].

The ILC is a class of adaptive algorithms, which improves the tracking accuracy of repetitive processes. The ILC is based on the idea that the information from previous trial is used to update the feedforward control law in order to obtain better performance of the assigned task on the next trial [5-7]. The following postulates are required for classical ILC [6,8]: every trail ends in a fixed time of duration, repetition of the initial setting (initial state coordinates) is satisfied, invariance of the system dynamics is ensured throughout the repetition, and the system output is measured in a deterministic way.

Linear iterative learning control (LILC) is an ILC for linear systems or based on a linear model of nonlinear systems [5,6]. If the linear approximation of a nonlinear dynamics results in great uncertainties, the corresponding LILC may fail to ensure the admissible tracking accuracy. In this case, one should resort to nonlinear models and nonlinear iterative learning control (NILC) [5,7]. In this paper, a nonlinear multiple-input-multiple-output (MIMO) dynamic model is considered. The ILC update-laws, proposed in [5] for linear or nonlinear dynamic systems, utilize learning operators which are constant gain-matrices or do not concern the robot dynamic model. Another approach to learning operator synthesis is based on the dynamic models with estimated parameters, respectively [9,10].

A classical off-line sampled-data ILC scheme for a plant with a sampled-data feedback controller attached is depicted in Fig. 2(a) [2] where sampled signals (dotted lines) from a continuous plant P are processed with the digital learning and feedback con-

trollers L and C, and where feedforward and feedback control signals (solid lines) are obtained by using a hold device H on the discrete-time signals generated by both controllers. So, the feedback and feedforward channels have equal sampling rate (Fig. 2(a)), and therefore, SD ILC is a particular case of the multirate ILC [2, 11] shown in Fig. 2 b), where the sampling rate for the feedback loop (dotted lines in Fig. 2(b)) is different than the sampling rate for the feedforward loop (dashed lines in Fig. 2(b)).

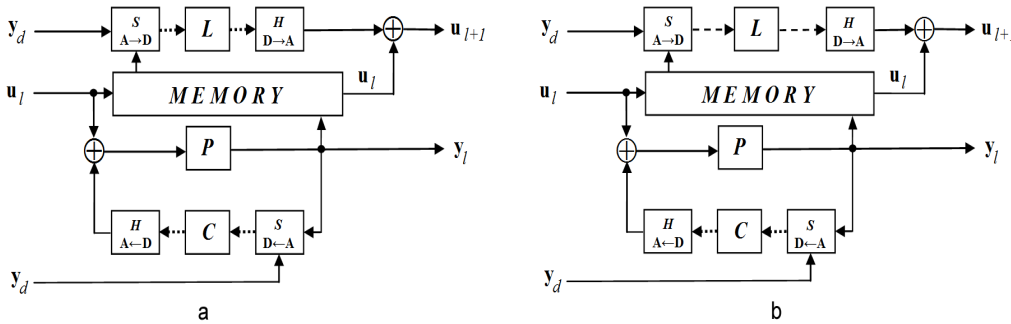

Figure 2. (a) Sampled-data ILC with a sampled-data feedback and sampled signals (dotted lines) have the same sampling rates ; (b) Multirate ILC - the sampling rate for the feedback loop (dotted lines) is different than the sampling rate for the feedforward loop (dashed lines).

In this paper we consider the special case of a continuous ILC for continuous nonlinear time-varying system (plant P in Fig. 3) with a sampled-data feedback controller attached. This case is applicable to ILC for robot manipulators with multi-joint arms with 4-6 degree of freedom (DOF) [9] or redundant kinematic structure [12]. This paper is aimed to present a model based nonlinear ILC with SD feedback and to prove the stability (uniform asymptotic convergence) of the new ILC law for robot manipulators, and to verify the proposed ILC algorithm by computer simulations of PUMA 560 robot manipulator.

The paper is organized as follows. Section 2 presents the design of a nonlinear ILC with a SD feedback for robot manipulators. Section 3 introduces the robustness and convergence analysis of the presented learning algorithm. The proposed ILC procedure with the SD feedback is validated and examined by computer simulation in Section 4.

2. Formulation of the problem

We consider robotic manipulator with n-DOF. The nonlinear multiple-input multiple-output (MIMO) dynamic model of the robot is based on the Lagrange's formulation of equations of motion in the space of generalized coordinates:

$$\mathbf{A}(\mathbf{q}_l)\ddot{\mathbf{q}}_l + \mathbf{b}(\mathbf{q}_l, \dot{\mathbf{q}}_l) + \mathbf{D}\dot{\mathbf{q}}_l + \mathbf{g}(\mathbf{q}_l) + \mathbf{f} = \mathbf{u} \tag{1}$$

where $l = 0, 1, \ldots, N$ is the iteration number, $\mathbf{q_l}$ is the $n \times 1$ vector of generalized coordinates (joint angles), $q_l^i \in [Q_i^*, Q_i^{**}]$, $i = 1, ..., n$, Q_i^{**} is the upper joint limit and Q_i^* is the lower joint limit of q_l^i; $\mathbf{A}(\mathbf{q}_l)$ is the $n \times n$ symmetric positive-definite inertia matrix; the $n \times 1$ vector $\mathbf{b}(\mathbf{q}_l, \dot{\mathbf{q}}_l)$ takes into account the Coriolis and centrifugal torques; $\mathbf{D} = \text{diag}\{\delta_1, \ldots, \delta_n\}$ denotes the diagonal $n \times n$ matrix of the coefficients of viscous friction; $\mathbf{g}(\mathbf{q}_l)$ is the $n \times 1$ vector representing gravity torques; $\mathbf{f} = [f_1 \text{sign}(\dot{q}_l^1) \ldots f_n \text{sign}(\dot{q}_l^n)]^{\text{T}}$ is the vector of coefficients of Coulomb friction and $\mathbf{u} = \mathbf{u}_l + \mathbf{u}_c$ is the $n \times 1$ vector of generalized torques where $\mathbf{u}_l$ and $\mathbf{u}_c$ are feedforward and feedback terms, respectively. The allowable set of generalized torques is a rectangular hyper-parallelepiped: $u_i \in [-U_i^{\max}, U_i^{\max}$; $U_i^{\max}$ and $-U_i^{\max}$ are the upper and lower limits of the control signal u_i.

The synthesis of an ILC with SD feedback consists of three steps: first, synthesis of an update control law, then, synthesis of a SD-feedback control law, and finally, specification of a learning operator. We assume the following notations: $h(\cdot) = h$ and $H(\cdot, \cdot) = H$, and $||\cdot||$ denotes Euclidean norm.

For the nonlinear MIMO dynamic model in equation (1), we propose the following feedforward update law:

$$\mathbf{u}_{l+1} = \mathbf{u}_l + \mathbf{L}[\ddot{\mathbf{q}}_d - \ddot{\mathbf{q}}_l + L_v(\dot{\mathbf{q}}_d - \dot{\mathbf{q}}_l) + L_p(\mathbf{q}_d - \mathbf{q}_l)] \tag{2}$$

where: $l = 0, 1, ..., N$ is the iteration number of the ILC procedure, $\mathbf{q_d}$ is an attainable and desired trajectory and $\mathbf{q_l}$ is the output trajectory at the lth iteration; $\mathbf{L} = \mathbf{L}(\mathbf{q}_l(t))$, is a learning operator; $\mathbf{u}_0 = \mathbf{u}_0(t)$ is the initial feed-forward control input; $t \ : \ t \in [0, T]$ is the tracking time and $[0, T]$ is the robot tracking time interval; L_v and L_p are learning control gains.

It has to be mentioned that, the calculation of $\mathbf{u}_{l+1}$ in Eq. (2) is offline and in the case of noisy measurements of $\mathbf{q}_l$ or $\dot{\mathbf{q}}_l$, a commonly used method is to low-pass filter the measured data and then differentiate the resultant signal.

Let us assume the following notations:

$$h(t_k) \equiv h^k, H(h^k) \equiv H^k, \{t_k : t_k = kt^s\}_{k=0}^K \subset [0, T], \ \ K = \lfloor T/t^s \rfloor$$

and

$$h^*(h^k, t) \equiv h^{*,t}, \ h^*(h^k, t) = \begin{cases} h^k, \ \forall t \in [t_k, t_{k+1}) \\ h^K, \ \forall t \in [t_K, T] \end{cases}, \quad k = 0, 1 \ldots K-1$$

is continuous piecewise-constant function on $[0, T]$, and t^s is the sampling interval. Then, we consider the following continuous piecewise-constant feedback control term [13]

$$\mathbf{u}_c^{*,t} \equiv \mathbf{u}_c^*(\mathbf{u}_c^k, t) : \mathbf{u}_c^k = \hat{\mathbf{A}}^k[\ddot{\mathbf{q}}_d^k + K_v(\dot{\mathbf{q}}_l^k - \dot{\mathbf{q}}_d^k) + K_p(\mathbf{q}_l^k - \mathbf{q}_d^k)] + \hat{\mathbf{b}}^k + \hat{\mathbf{D}}\dot{\mathbf{q}}_l^k + \hat{\mathbf{g}}^k + \hat{\mathbf{f}}^k \tag{3}$$

where: $\hat{\mathbf{A}}^k = \hat{\mathbf{A}}(\mathbf{q}(t_k))$ and $\hat{\mathbf{A}}$ is an estimate of the inertia matrix $\mathbf{A}$, obtained by a parameter identification technique, $\hat{\mathbf{b}}^k$, $\hat{\mathbf{D}}$, $\hat{\mathbf{g}}^k$, and $\hat{\mathbf{f}}^k$ are the corresponding estimates of $\mathbf{b}^k$, $\mathbf{D}$, $\mathbf{g}^k$, and $\mathbf{f}^k$; K_v and K_p are the feedback gains.

Usually, the learning operator should be selected to satisfy a sufficient condition for convergence of the ILC algorithm [5,9]. Therefore, the third step (learning operator selection) of the ILC synthesis will be completed after the proof of the learning convergence.

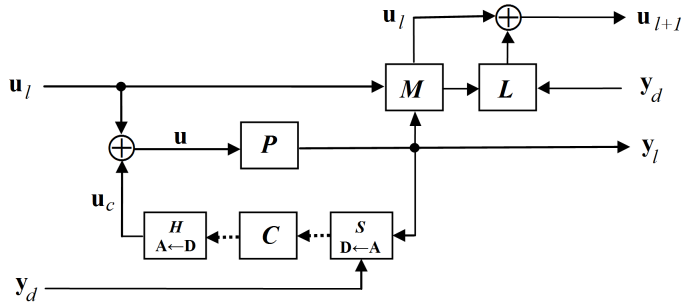

Figure 3. Continuous-time ILC scheme with sampled-data feedback.

Equations (1), (2) and (3) describe the following classical off-line ILC scheme with SD feedback depicted in Fig. 3 where **P** represents the robot arm; **C** and **L** are feedback and feed-forward controllers, respectively; **M** is the memory of the control system; the input trajectory $\mathbf{u}_i$ is the feed-forward term of the control law $\mathbf{u} = \mathbf{u}_l + \mathbf{u}_c$ and $l = 0, 1, ..., N$ is the current iteration number; $\mathbf{q}_l$ is the actual output trajectory; $\mathbf{q}_d$ is the desired output trajectory; **S** and **H** are the sampler and the holder, correspondingly. The off-line computed feed forward term $\mathbf{u}_{i+1}$ improves the tracking performance of the robot on the next iteration.

In contrast to the SD ILC and multirate ILC schemes shown in Fig. 2(a) and 2(b), we assume that the proposed ILC (Fig. 3) is continuous because of the following reasons:

- The digital ILC controller (computer) calculates off-line the feedforward control term. Therefore, the discretization frequency (sampling rate) of the output of the learning controller could be as high as needed. For example, if the robot actuators are controlled by a PWM (Pulse Width Modulation) signal, the sampling rate of the feedforward control output faster than the duty cycle command rate of the PWM will not be reflected in the PWM output [14] and the feedforward output could be assumed as a continuous one.

- The ILC systems with input and output signals that are transmitted through a communication network (networked ILC systems [3]) require a sampled-data or a multirate ILC, but this is not the typical case of industrial robot applications. That's why we don't consider networked ILC systems in this paper.

- Recently, several multirate ILC schemes have been proposed to guarantee good learning transient (acceptable transient error) [11]. As the learning transient (transient growth) is the major problem for the applicability of a nonlinear ILC [15],

we use the bounded error ILC algorithm [10] in order to solve this problem in a safe, fast and simple manner and consequently multirate ILC schemes are not needed to solve the learning transient problem.

It has to be mentioned that the output signal of the feedback controller, depicted by dotted line in Fig. 3, has not to be assumed as a continuous one because it has to be calculated online in real-time. Moreover, the calculation time of the feedback, generated by the proposed model based (dynamics based) controller in Eq. (3), cannot be neglected especially for a multi-joint robotic arm and a zero-order holder which generates a piecewise constant signal (staircase signal) must be used.

3. Convergence and robustness of the learning control with a sampled-data feedback

In this section we present the main result of this paper, that is, the proof of the robustness and convergence of the proposed ILC scheme with a sampled-data feedback.

3.1. A sufficient condition for convergence and robustness of ILC for a class of nonlinear time-varying systems

We consider a class of multi-input-multi-output nonlinear time-varying systems described by the following state-space equations [16,17]:

$$\begin{aligned} \dot{\mathbf{x}}_l(t) &= f(\mathbf{x}_l(t),t) + B(\mathbf{x}_l(t),t)\mathbf{u}_l(t) + \omega_l(t) \\ \mathbf{y}_l(t) &= g(\mathbf{x}_l(t),t) \end{aligned} \tag{4}$$

where, for $l \in \{0,1...,\infty\}$ and all $t \in [0,T]$, $\mathbf{x}_l(t) \in \Re^n$, $\mathbf{y}_l(t) \in \Re^m$, $\mathbf{u}_l(t) \in \Re^r$ are not necessarily continuous, and $\omega_l(t) \in \Re^n$ represents both deterministic and random disturbances. The functions $f : \Re^n \times [0,T] \to \Re^n$ and $B : \Re^n \times [0,T] \to \Re^{n\times r}$ are piecewise continuous in $t \in [0,T]$ and $g : \Re^n \times [0,T] \to \Re^m$ is differentiable in $\mathbf{x}$ and t, with partial derivatives $g_x(\cdot,\cdot)$ and $g_t(\cdot,\cdot)$. In addition, the following assumptions hold [16,17]:

I. For each fixed initial state $\mathbf{x}(0)$ with $\omega(\cdot) \equiv 0$ the output map $O : C([0,T],\Re^r) \times \Re^n \to C([0,T],\Re^m)$ and the state map $S : C([0,T],\Re^r) \times \Re^n \to C([0,T],\Re^n)$ are one-to-one. In this notation $\mathbf{y}_l(\cdot) = O(\mathbf{u}_l(\cdot),\mathbf{x}_l(0))$ and $\mathbf{x}_l(\cdot) = S(\mathbf{u}_l(\cdot),\mathbf{x}_l(0))$.

II. The disturbance $\omega_l(\cdot)$ is bounded on $[0,T]$ i.e. $\|\omega(t)\| \leqslant b_\omega$.

III. The functions $f(\cdot,\cdot)$, $B(\cdot,\cdot)$, $g_x(\cdot,\cdot)$, and $g_t(\cdot,\cdot)$ are uniformly globally Lipschitz in $\mathbf{x}$ on the interval $[0,T]$.

IV. The operators $B(\cdot,\cdot)$ and $g_x(\cdot,\cdot)$ are bounded on $[0,T] \times \Re^n$.

V. All functions are assumed measurable and integrable.

Let us consider the following learning update law

$$\mathbf{u}_{l+1}(t) = (1-\gamma)\mathbf{u}_l + \gamma\mathbf{u}_0 + L(\mathbf{y}_l,t)(\dot{\mathbf{y}}_d - \dot{\mathbf{y}}_l) \tag{5}$$

where $L : \Re^m \times [0,T] \to \Re^{r\times m}$ is a bounded learning operator, $\mathbf{y}_d(t) \equiv \mathbf{y}_0(t)$ and $\gamma \in [0.1)$ allows the influence of a bias term [16]. Equation (5) describes a standard D-type (Differential-type) NLIC for a class of nonlinear time-varying systems (Eq. (4)), with a nonlinear time-varying learning operator.

Lemma 3 [16] *If* $\{a_l\}$, $l \in \{0,1...,\infty\}$ *is a sequence of real numbers such that* $|a_{l+1}| \leqslant \rho\,|a_l| + \varepsilon$, $0 \leqslant \rho < 1$, *then* $\limsup_{l\to\infty} |a_l| \leqslant (1-\rho)^{-1}\varepsilon$.

The proof of Lemma 1 is presented in [16].

We define the time-weighted norm (λ norm) for a function $h(t)$, $t \in [0,T]$ by $\|h(t)\|_\lambda = \sup_{t\in[0,T]} e^{-\lambda t}\,\|h(t)\|$.

Lemma 4 *If* h^k *is a discrete form of* $h(t)$, $t \in [0,T]$ $(h^k = h(t_k),\ \{t_k : t_k = kt^s\}_{k=0}^K \subset [0,T])$ *and* $h^{*,t}$ *is the corresponding continuous piecewise-constant function on* $[0,T]$, *then* $\|h^{*,t}\|_\lambda \leqslant \|h(t)\|_\lambda$.

The proof of Lemma 2 is presented in Appendix 1.

Theorem 4 [16,17] *Let the system described by equation* (3) *satisfy Assumptions* I-V *and use the update law in Eq.* (5). *Given an attainable desired trajectory* $\mathbf{y}_d(t) = g(\mathbf{x}_d(t),t), t \in [0,\mathrm{T}]$, $\mathbf{u}_d(t)$ *is the corresponding input and* $\mathbf{x}_d(t)$ *is the corresponding state (according to* I*). If*

$$\|(1-\gamma)\mathbf{I} - L(g(\mathbf{x},t),t)g_x(\mathbf{x},t)B(\mathbf{x},t\,)\| \leqslant \rho < 1\ ,\ \forall(\mathbf{x},t) \in \mathbf{R}^n \times [0,T] \tag{6}$$

and the initial state error $\|x_d(0) - x_l(0\,)\|$ *is bounded by* b_{x0}, *then, as* $l \to \infty$, *the error between* $\mathbf{u}_l(t)$ *and* $\mathbf{u}_d(t)$ *is bounded. In addition, the state and output asymptotic errors are bounded. These bounds depend continuously on the bound on the initial state error, bound on the state disturbance, and* γ, *as* b_{x0}, b_ω, *and* γ *tend to zero, these bounds also tend to zero.*

The proof of Theorem 1 for continuous systems (see Eq. (4)) is presented in [16,17]. Consequently, the learning operator remains to be specified so that the sufficient condition for robustness and convergence, Eq. (6), to hold.

Corollary 1 [16] *If the update law* (5) *is replaced with*

$$\mathbf{u}_{l+1}(t) = (1-\gamma)\mathbf{u}_l + \gamma\mathbf{u}_0 + L(\mathbf{y}_l,t)(\dot{\mathbf{y}}_d - \dot{\mathbf{y}}_l) + K(\mathbf{y}_l,t)(\mathbf{y}_d - \mathbf{y}_l) \tag{7}$$

with $K(\cdot,\cdot)$ *bounded, then Theorem* 1 *still holds.*

The proof of Corollary 1 is presented in [16]. Equation (7) describes a PD-type ILC.

It has to be mentioned that for robust convergence the update law (7) and (5) must contain derivatives of the output $\dot{\mathbf{y}}_d - \dot{\mathbf{y}}_l$ [16].

In all practical cases of robotic manipulators the input signal belongs to a compact subset $u_i \in [-U_i^{\max}, U_i^{\max}]$ and the output trajectory belongs to the subset $q_l^i \in [Q_i^*, Q_i^{**}]$, $i = 1, ..., n$. If the ILC update law (see Eq. (3)) produces a feedforward input that is out of the allowable compact set of inputs, and this set is a convex set, then projecting back into the allowable set ensures the validity of Theorem 1 [16]. If the output trajectories are out of the corresponding allowable set due to trajectory errors, then an application of the 'Bounded-error algorithm' presented in [10] can solve this problem for NILC.

3.2. A sufficient condition for convergence and robustness of the ILC with the SD feedback for robot manipulators

In this subsection we present the proof of the robustness and convergence of the proposed ILC scheme with a sampled-data feedback. The main idea is to prove Theorem 1 for the considered ILC design with the SD feedback.

$$\begin{pmatrix} \dot{\mathbf{q}}_l \\ \ddot{\mathbf{q}}_l \end{pmatrix} = \begin{pmatrix} \dot{\mathbf{q}}_l \\ -\mathbf{A}^{-1}(\mathbf{b} + \mathbf{D}\dot{\mathbf{q}}_l + \mathbf{g}) \end{pmatrix} + \begin{pmatrix} 0 \\ \mathbf{A}^{-1} \end{pmatrix} \mathbf{u}_c^{*,t} + \begin{pmatrix} 0 \\ -\mathbf{A}^{-1} \end{pmatrix} \mathbf{f} + \begin{pmatrix} 0 \\ \mathbf{A}^{-1} \end{pmatrix} \mathbf{u}_l. \quad (8)$$

Let us define

$$\dot{\mathbf{x}}_l = \begin{pmatrix} \dot{\mathbf{q}}_l \\ \ddot{\mathbf{q}}_l \end{pmatrix} \quad f = f_1(\mathbf{q}_l, \dot{\mathbf{q}}_l) + B(\mathbf{q}_l) f_2^{*,t}(\mathbf{q}_l^k, \dot{\mathbf{q}}_l^k), \quad f_1 = \begin{pmatrix} \dot{\mathbf{q}}_l \\ -\mathbf{A}^{-1}(\mathbf{b} + \mathbf{D}\dot{\mathbf{q}}_l + \mathbf{g}) \end{pmatrix}$$

and

$$f_2^{*,t} \equiv f_2^*(f_2^k, t) : f_2^k = \hat{\mathbf{A}}^k(\ddot{\mathbf{q}}_d^k + K_v(\dot{\mathbf{q}}_l^k - \dot{\mathbf{q}}_d^k) + K_p(\mathbf{q}_l^k - \mathbf{q}_d^k)) + \hat{\mathbf{b}}^k + \hat{\mathbf{D}}\dot{\mathbf{q}}_l^k + \hat{\mathbf{g}}^k \quad (9)$$

$B = \begin{pmatrix} 0 \\ \mathbf{A}^{-1} \end{pmatrix}$, and $\mathbf{y}_l = \mathbf{x}_l$. Thus, treating the Coulumb friction as a disturbance $\omega_l = \begin{pmatrix} 0 \\ -\mathbf{A}^{-1} \end{pmatrix} (\mathbf{f} - \hat{\mathbf{f}})$, from equation (8) we obtain equation (4) for $r = m = n$.

Let us consider the continuous feedback control law proposed in [13] which corresponds to the discrete feedback law defined by Eq. (3):

$$\mathbf{u}_c(\mathbf{q}_l, \dot{\mathbf{q}}_l, t) = \hat{\mathbf{A}}[\ddot{\mathbf{q}}_d + K_v(\dot{\mathbf{q}}_l - \dot{\mathbf{q}}_d) + K_p(\mathbf{q}_l - \mathbf{q}_d)] + \hat{\mathbf{b}} + \hat{\mathbf{D}}\dot{\mathbf{q}}_l + \hat{\mathbf{g}} + \hat{\mathbf{f}}. \quad (10)$$

Using Eq. (9) and Eq. (10) we obtain the continuous form of $f_2^{*,t}$

$$f_2 = \hat{\mathbf{A}}[\ddot{\mathbf{q}}_d + K_v(\dot{\mathbf{q}}_l - \dot{\mathbf{q}}_d) + K_p(\mathbf{q}_l - \mathbf{q}_d)] + \hat{\mathbf{b}} + \hat{\mathbf{D}}\dot{\mathbf{q}}_l + \hat{\mathbf{g}}. \quad (11)$$

To apply Theorem 1 we need to check that Assumptions I-V are satisfied. In [16] it is proven that f_1, f_2 and B satisfy Assumptions I-V, and consequently, we can apply

Theorem 1 to the system in Eq. (8) with the continuous feedback given by Eq. (10) and the update law in Eq. (2). Thus, to prove the convergence of the considered ILC scheme with the SD feedback we have to prove Theorem 1 for the continuous piecewise-constant feedback control law in Eq. (3).

Let us define $\delta\mathbf{u}_l \equiv \mathbf{u}_d(t) - \mathbf{u}_l(t)$ and $\delta\dot{\mathbf{y}}_l \equiv \dot{\mathbf{y}}_d(t) - \dot{\mathbf{y}}_l(t)$. Because in all practical cases the input signal belongs to a compact subset of $\Re^r$ further we will consider that $\mathbf{u}_l(t), t \in [0,T] : \|\mathbf{u}_l(t)\|_\infty \leqslant b_u$ where $\|\mathbf{u}_l(t)\|_\infty = \sup_{t\in[0,T]} \|\mathbf{u}_l(t)\|$ is the supremum norm.

For simplification, we introduce the following notations:

$$\begin{aligned}
&\mathbf{x}_l \equiv \mathbf{x}_l(t) && \mathbf{x}_d \equiv \mathbf{x}_d(t)\\
&\mathbf{y}_l \equiv \mathbf{y}_l(t) && \mathbf{y}_d \equiv \mathbf{y}_d(t)\\
&\mathbf{u}_l \equiv \mathbf{u}_l(t) && \mathbf{u}_d \equiv \mathbf{u}_d(t)\\
&\omega_l \equiv \omega_l(t)\\
&f_l \equiv f_l(\mathbf{x}_l(t),t) && f_d \equiv f_d(\mathbf{x}_d(t),t)\\
&B_l \equiv B_l(\mathbf{x}_l(t),t) && B_d \equiv B_d(\mathbf{x}_d(t),t)\\
&g_{xl} \equiv \frac{\partial}{\partial \mathbf{x}} g(\mathbf{x}(t),t)\Big|_{\mathbf{x}=\mathbf{x}_l(t)} && g_{xd} \equiv \frac{\partial}{\partial \mathbf{x}} g(\mathbf{x}(t),t)\Big|_{\mathbf{x}=\mathbf{x}_d(t)}\\
&g_{tl} \equiv \frac{\partial}{\partial t} g(\mathbf{x}(t),t)\Big|_{\mathbf{x}=\mathbf{x}_l(t)} && g_{td} \equiv \frac{\partial}{\partial t} g(\mathbf{x}(t),t)\Big|_{\mathbf{x}=\mathbf{x}_d(t)}
\end{aligned}$$

and k_{gx}, k_{gt}, k_f, k_B are Lipschitz constants for $g_x(\cdot,\cdot)$, $g_t(\cdot,\cdot)$, $f(\cdot,\cdot)$ and $B(\cdot,\cdot)$ respectively, and b_{gx}, b_{ud}, b_{f2d}, b_L and b_B are the corresponding norm bounds on $g_x(\cdot,\cdot)$, $\mathbf{u}_d(\cdot)$, $f_{d2}^{*,t}(\cdot,\cdot)$, $L(\cdot,\cdot)$ and $B(\cdot,\cdot)$.

Now we proceed to prove a sufficient condition for convergence and robustness of the ILC with the SD feedback for robot manipulators described in Eqs. (8), (5) and (3).

Theorem 5 *Let the system of robot dynamics with a SD feedback controller attached is described by the state-space equations in* (8) *where the feedback control law is given by Eq.* (9) *with the piecewise-continuous function* $f_2^{*,t}$ *and the function* f_2 *in Eq.* (11) *is the continuous form of* $f_2^{*,t}$. *If the system in* (8) *with* $f = f_1(\mathbf{q}_l, \dot{\mathbf{q}}_l) + B(\mathbf{q}_l) f_2(\mathbf{q}_l, \dot{\mathbf{q}}_l)$, *i.e. – the feedback control is given by* f_2 *in Eq.* (11), *satisfies Assumptions* I-V *and the sufficient condition* (6) *for robustness and convergence of the ILC law* (5) *is satisfied, then the Theorem* 1 *also holds for the system* (8) *with SD feedback given by* $f_2^{*,t}$ *in Eq.* (9) *and the ILC update law in* (5).

Proof From Eq. (5) it follows

$$\delta\mathbf{u}_{l+1} = \mathbf{u}_d - (1-\gamma)\mathbf{u}_l - \gamma\mathbf{u}_0 - L\delta\dot{\mathbf{y}}_l. \tag{12}$$

Using the above notations for $\delta\dot{\mathbf{y}}_l$ from Eq. (4) we obtain:

$$\delta\dot{\mathbf{y}}_l = g_{xd}(f_d + B_d\mathbf{u}_d) + g_{td} - g_{xl}(f_l + B_l\mathbf{u}_l + \omega_l) - g_{tl}. \tag{13}$$

Combining Eq. (13) with $g_{xl}(f_d + B_d\mathbf{u}_d + B_l f_{d2}^{*,t}) - g_{xl}(f_d + B_d\mathbf{u}_d + B_l f_{d2}^{*,t})$, $g_{xl}(B_l\mathbf{u}_d - B_l\mathbf{u}_d)$, $f_l = f_{l1} + B_l f_{l2}^{*,t}$ and $f_d = f_{d1} + B_d f_{d2}^{*,t}$ yields

$$\begin{aligned} \delta\dot{\mathbf{y}}_l &= (g_{xd} - g_{xl})(f_d + B_d\mathbf{u}_d) + g_{xl}(f_{d1} - f_{l1}) + g_{xl}B_l(f_{d2}^{*,t} - f_{l2}^{*,t}) \\ &+ g_{xl}(B_d - B_l)(\mathbf{u}_d + f_{d2}^{*,t}) + g_{xl}B_l(\delta\mathbf{u}_l) + (g_{td} - g_{tl}) - g_{xl}\omega_l. \end{aligned} \tag{14}$$

Combining Eq. (12) with $\gamma\mathbf{u}_d - \gamma\mathbf{u}_d$ and Eq. (14) yields

$$\delta\mathbf{u}_{l+1} = (1-\gamma)\delta\mathbf{u}_l + \gamma\delta\mathbf{u}_0 - L\begin{bmatrix} g_{xl}B_l(\delta\mathbf{u}_l) + (g_{xd} - g_{xl})(f_d + B_d\mathbf{u}_d) \\ + g_{xl}(f_{d1} - f_{l1}) + g_{xl}B_l(f_{d2}^{*,t} - f_{l2}^{*,t}) \\ + g_{xl}(B_d - B_l)(\mathbf{u}_d + f_{d2}^{*,t}) \\ + (g_{td} - g_{tl}) - g_{xl}\omega_l \end{bmatrix}. \tag{15}$$

Taking norms, using the bounds and using the Lipschitz conditions (see assumptions II-IV) from Eq. (15) we obtain:

$$\begin{aligned} &\|\delta\mathbf{u}_{l+1}\| \leqslant \|(1-\gamma)\mathbf{I} - Lg_{xl}B_l\|\,\|\delta\mathbf{u}_l\| + \gamma\|\delta\mathbf{u}_0\| \\ &+ b_L\left[(k_{gx}b_d + k_{gt} + b_{gx}(k_{f1} + k_B(b_{ud} + b_{f2d})))\,\|\delta\mathbf{x}_l\| + k_{f2}b_{gx}b_B\left\|\delta\mathbf{x}_l^{*,t}\right\| + b_{gx}b_\omega\right]. \end{aligned} \tag{16}$$

Multiplying (16) by $e^{-\lambda t}$, defining $k_1 = b_L(k_{gx}b_d + k_{gt} + b_{gx}(k_{f1} + k_B(b_{ud} + b_{f2d})))$, $k_2 = b_L k_{f2}b_{gx}b_B$ and $k_3 = b_L b_{gx}$, and assuming the sufficient condition for convergence (6) the inequality (16) simplifies to

$$\begin{aligned} &e^{-\lambda t}\|\delta\mathbf{u}_{l+1}\| \\ &\quad\leqslant \rho e^{-\lambda t}\|\delta\mathbf{u}_l\| + \gamma e^{-\lambda t}\|\delta\mathbf{u}_0\| + k_1 e^{-\lambda t}\|\delta\mathbf{x}_l\| + k_2 e^{-\lambda t}\left\|\delta\mathbf{x}_l^{*,t}\right\| + k_3 e^{-\lambda t}b_\omega. \end{aligned} \tag{17}$$

Taking the supremum of both sides of (17) and applying Lemma 2 to $\delta\mathbf{x}_l^{*,t}$ yields

$$\begin{aligned} \sup_{t\in[0,T]} e^{-\lambda t}\|\delta\mathbf{u}_{l+1}\| &\leqslant \rho \sup_{t\in[0,T]} e^{-\lambda t}\|\delta\mathbf{u}_l\| + \gamma \sup_{t\in[0,T]} e^{-\lambda t}\|\delta\mathbf{u}_0\| \\ &+ (k_1 + k_2)\sup_{t\in[0,T]} e^{-\lambda t}\|\delta\mathbf{x}_l\| + k_3 b_\omega. \end{aligned} \tag{18}$$

Using the time-weighted norm definition and defining $k = k_1 + k_2$ from (18) we obtain

$$\|\delta\mathbf{u}_{l+1}\|_\lambda \leqslant \rho\|\delta\mathbf{u}_l\|_\lambda + \gamma\|\delta\mathbf{u}_0\|_\lambda + k\|\delta\mathbf{x}_l\|_\lambda + k_3 b_\omega. \tag{19}$$

On the other hand, using the integral expression

$$\mathbf{x}_l(t) = \mathbf{x}_l(0) + \int_o^t (B(\mathbf{x}_l(\tau),\tau)\mathbf{u}_l(\tau) + f(\mathbf{x}_l(\tau),\tau) + \omega_l(\tau))d\tau$$

where $f(\mathbf{x}(t),t) = f_1(\mathbf{x}(t),t) + B(\mathbf{x}(t),t)f_2^{*,t}(\mathbf{x}(t),t)$ and $f_2^{*,t}(\mathbf{x}(t),t)$, $t \in [0,T]$ is continuous piecewise-constant function, and taking norms for $\|\delta\mathbf{x}_l\|$ we have

$$\begin{aligned}\|\delta\mathbf{x}_l\| \leqslant \|\delta\mathbf{x}_l(0)\| + \int_o^t \|B_d\mathbf{u}_d - B_l\mathbf{u}_l\|d\tau + \int_o^t \|f_{1d} - f_{1l}\|d\tau \\ + \int_o^t \left\|B_d f_{2d}^{*,\tau} - B_l f_{2l}^{*,\tau}\right\|d\tau + \int_o^t \|\omega_l\|\, d\tau.\end{aligned} \tag{20}$$

Adding $B_l f_{d2}^{*,t} - B_l f_{d2}^{*,t}$ and $B_l\mathbf{u}_d - B_l\mathbf{u}_d$ to Eq. (20), and using the bounds, and the Lipschitz conditions yields

$$\|\delta\mathbf{x}_l\| \leqslant \|\delta\mathbf{x}_l(0)\| + b_B\int_o^t \|\delta\mathbf{u}_l\|\, d\tau + k_4\int_o^t \|\delta\mathbf{x}_l\|\, d\tau + k_5\int_o^t \left\|\delta\mathbf{x}_l^{*,\tau}\right\| d\tau + b_\omega t \tag{21}$$

where $k_4 = (k_B(b_{ud} + b_{f2d}) + k_{f1})$ and $k_5 = b_B k_{f2}$. Multiplying (21) by $e^{-\lambda t}$ we have that

$$\begin{aligned}e^{-\lambda t}\|\delta\mathbf{x}_l\| \leqslant e^{-\lambda t}\|\delta\mathbf{x}_l(0)\| + b_B e^{-\lambda t}\int_o^t e^{-\lambda\tau}\|\delta\mathbf{u}_l\|\, e^{\lambda\tau}d\tau \\ + k_4 e^{-\lambda t}\int_o^t e^{-\lambda\tau}\|\delta\mathbf{x}_l\|\, e^{\lambda\tau}d\tau + k_5 e^{-\lambda t}\int_o^t e^{-\lambda\tau}\left\|\delta\mathbf{x}_l^{*,\tau}\right\| e^{\lambda\tau}d\tau + b_\omega t e^{-\lambda t}.\end{aligned} \tag{22}$$

Noticing that $e^{-\lambda t}$ is always of the same sign and $\sup_{t\in[0,T]} e^{-\lambda t}\left\|\delta\mathbf{x}_l^{*,t}(t)\right\| \leqslant \sup_{t\in[0,T]} e^{-\lambda t}\|\delta\mathbf{x}_l(t)\|$, (see Lemma 2), and applying the Second Mean Value Theorem for Integrals [18] to the integral expressions in inequality (22) yields:

$$\begin{aligned}e^{-\lambda t}\|\delta\mathbf{x}_l\| \leqslant e^{-\lambda t}\|\delta\mathbf{x}_l(0)\| + b_B e^{-\lambda t}\sup_{\tau\in[0,t]} e^{-\lambda\tau}\|\delta\mathbf{u}_l\|\int_o^t e^{\lambda\tau}d\tau \\ + \left[k_4 e^{-\lambda t}\sup_{\tau\in[0,t]} e^{-\lambda\tau}\|\delta\mathbf{x}_l\| + k_5 e^{-\lambda t}\sup_{\tau\in[0,t]} e^{-\lambda\tau}\|\delta\mathbf{x}_l\|\right]\int_o^t e^{\lambda\tau}d\tau + b_\omega t e^{-\lambda t}.\end{aligned} \tag{23}$$

Taking into account that $\sup_{\tau\in[0,t]} e^{-\lambda\tau}\|\delta\mathbf{x}_l\| \leqslant \sup_{t\in[0,T]} e^{-\lambda t}\|\delta\mathbf{x}_l\|$, $t\in[0,T]$ and taking the supremum of both sides of (23) we have that

$$\|\delta\mathbf{x}_l\|_\lambda \leqslant \|\delta\mathbf{x}_l(0)\|_\lambda + b_B(1-e^{-\lambda T})\lambda^{-1}\|\delta\mathbf{u}_l\|_\lambda + k_6(1-e^{-\lambda T})\lambda^{-1}\|\delta\mathbf{x}_l\|_\lambda + b_\omega T \quad (24)$$

where $k_6 = k_4 + k_5$. Thus, from inequality (24) we obtain

$$\begin{aligned}\|\delta\mathbf{x}_l\|_\lambda &\leqslant \lambda(\lambda - k_6(1-e^{-\lambda T}))^{-1}\|\delta\mathbf{x}_l(0)\|_\lambda \\ &\quad + b_B(1-e^{-\lambda T})(\lambda - k_6(1-e^{-\lambda T}))^{-1}\|\delta\mathbf{u}_l\|_\lambda + \lambda T(\lambda - k_6(1-e^{-\lambda T}))^{-1}b_\omega.\end{aligned} \quad (25)$$

Combining inequalities (19) and (25) yields

$$\begin{aligned}\|\delta\mathbf{u}_{l+1}\|_\lambda &\leqslant \frac{k\lambda}{\lambda - k_6(1-e^{-\lambda T})}\|\delta\mathbf{x}_l(0)\|_\lambda \\ &\quad + \left[\rho + \frac{kb_B(1-e^{-\lambda T})}{\lambda - k_6(1-e^{-\lambda T})}\right]\|\delta\mathbf{u}_l\|_\lambda + \left[k_3 + \frac{k\lambda T}{\lambda - k_6(1-e^{-\lambda T})}\right]b_\omega + \gamma\|\delta\mathbf{u}_0\|_\lambda.\end{aligned} \quad (26)$$

Defining $\bar\rho = \rho + kb_B(1-e^{-\lambda T})(\lambda - k_6(1-e^{-\lambda T}))^{-1}$, $k_7 = k\lambda(\lambda - k_6(1-e^{-\lambda T}))^{-1}$, $k_8 = (k_3 + k\lambda T(\lambda - k_6(1-e^{-\lambda T}))^{-1})$ and $\varepsilon = k_7\|\delta\mathbf{x}_l(0)\|_\lambda + k_8 b_\omega + \gamma\|\delta\mathbf{u}_0\|_\lambda$ we have that

$$\|\delta\mathbf{u}_{l+1}\|_\lambda \leqslant \bar\rho\|\delta\mathbf{u}_l\|_\lambda + \varepsilon. \quad (27)$$

Since $\rho < 1$ we can find $\lambda > k_6(1-e^{-\lambda T}) : \bar\rho < 1$. Thus we can apply Lemma 1 so that

$$\limsup_{l\to\infty}\|\delta\mathbf{u}_{l+1}\|_\lambda \leqslant (1-\bar\rho)^{-1}\varepsilon \quad (28)$$

implying that $\mathbf{u}_l$ converges to $\mathbf{u}_d$ when $l\to\infty$, $\|\delta\mathbf{x}_l(0)\|\to 0$, $b_\omega\to 0$ and $\gamma\to 0$ implying that $\varepsilon\to 0$. □

It has to be mentioned that all corollaries of Theorem 1 proven in [16] for continuous-time systems are also valid for Theorem 2 (for nonlinear time-varying systems with sampled-data feedback) implying that the Corollary 1 holds and the proposed ILC update law (2) is robust and convergent if the sufficient condition for convergence (6) is satisfied.

The main contribution of Theorem 2 is that it proves the asymptotic convergence of ILC with Sampled-Data feedback controller, because only the asymptotic convergence of an ILC can assure its practical implementation. Thus, applying Theorem 2 to prove the convergence of considered ILC algorithm with SD feedback, for the nonlinear system in Eq. (8) one can obtain from Eq. (6) the simplest ($\gamma = 0$, $\mathbf{y}_l \equiv \mathbf{x}_l$) sufficient condition for convergence of the proposed ILC design for robotic manipulators [16]:

$$\left\|\mathbf{I} - \mathbf{L}\mathbf{A}^{-1}\right\| \leqslant \rho < 1 \quad (29)$$

where $\mathbf{I}$ is the identity matrix of size n.

From Eq. (12), following Arimoto's ideas in [5] for better convergence rate, we consider a learning operator to be as close as possible to the inertia matrix. Therefore, we propose the learning operator to be identically equal to $\hat{\mathbf{A}}$, i.e. - $\mathbf{L} \equiv \hat{\mathbf{A}}$ [9]. Thus, the last (third) step of the ILC synthesis for robotic manipulators is completed by specification of the learning operator.

4. Simulation results

In this section, we present the simulation results from implementation of the ILC with SD feedback described in the previous sections. We consider the dynamic model of PUMA 560, 6 DOF, robot reported in [19] and given by Eq. (1).

For a realistic computer simulation of parameter uncertainty we are going to use two sets of model parameters. We assume the explicit dynamic model of PUMA560 robot arm (left-hand side of the Eq. (1)) with parameters reported by Armstrong et al. [19], Corke, and Armstrong-Helouvry [20]. This first set of model parameters is described in Tab. 1 and we consider them as virtual parameters $\xi = (\xi_1^i, ..., \xi_{13}^i)$, $i = 1, ..., 6$, where i corresponds to the link number.

For the learning-control-input synthesis, we assume the PUMA 560 model parameters estimated by Tarn et al. [21]. This second set of parameters, pointed out as $\hat{\xi} = (\hat{\xi}_1^i, ..., \hat{\xi}_{14}^i)$, $i = 1, ..., 6$, is shown in Tab. 2 and we consider it as the set of identification estimates of the virtual parameters.

Let the desired trajectory be given in generalized (joint) coordinates by:

$$\begin{aligned} &q_d^1(t) \equiv 0 && q_d^2(t) = -2\cos(4t) + 2 && q_d^3(t) = -\cos(4t) + 1 \\ &q_d^4(t) = -3\cos(4t) + 3 && q_d^5(t) = -1.5\cos(4t) + 1.5 && q_d^6(t) \equiv 0 \end{aligned} \tag{30}$$

and $t \in [0, 0.25\pi]$. Thus, for $q_l^i \in [-2\pi, 2\pi]$, $i = 1, 2..., 6$, $\mathbf{L} \equiv \hat{\mathbf{A}}$, combining Eq. (1) with Eq. (2) and Eq. (3) yields the control law of the proposed NILC with SD feedback:

$$\begin{aligned} \mathbf{A}\ddot{\mathbf{q}}_{l+1} + \mathbf{b} + \mathbf{D}\dot{\mathbf{q}}_{l+1} + \mathbf{g} + \mathbf{f} = \mathbf{u}_l + \hat{\mathbf{A}}[\ddot{\mathbf{q}}_d - \ddot{\mathbf{q}}_l + L_v(\dot{\mathbf{q}}_d - \dot{\mathbf{q}}_l) + L_p(\mathbf{q}_d - \mathbf{q}_l)] \\ + \hat{\mathbf{A}}^k[\ddot{\mathbf{q}}_d^k + K_v(\dot{\mathbf{q}}_{l+1}^k - \dot{\mathbf{q}}_d^k) + K_p(\mathbf{q}_{l+1}^k - \mathbf{q}_d^k)] + \hat{\mathbf{b}}^k + \hat{\mathbf{D}}\dot{\mathbf{q}}_{l+1}^k + \hat{\mathbf{g}}^k + \hat{\mathbf{f}}^k \end{aligned} \tag{31}$$

where $l \in \{0, 1..., N\}$, $\hat{\mathbf{A}}, \hat{\mathbf{b}}, \hat{\mathbf{D}}$, $\hat{\mathbf{g}}$ and $\hat{\mathbf{f}}$, calculated by using parameters in Tab. 2, are the corresponding estimates of $\mathbf{A}, \mathbf{b}, \mathbf{D}$, $\mathbf{g}$, and $\mathbf{f}$ in Eq. (1), calculated by using parameters in Tab. 1.

We are able to validate inequality (29) for $q_l^i \in [-2\pi, 2\pi]$, $i = 1, ..., 6$. A computation of the maximum of the left-hand side of (29) results in: $\max_{q_l^i} \left\| \mathbf{I} - \hat{\mathbf{A}}(\mathbf{q}_l, \hat{\xi})\mathbf{A}^{-1}(\mathbf{q}_l, \xi) \right\| \approx$ 0.6013 with a tolerance of ± 0.0018 and consequently the sufficient condition for convergence (29) holds with respect to $q_l^i \in [-2\pi, 2\pi]$, $i = 1, ..., 6$, and the NILC procedure proposed in Eq. (31) is convergent.

Table 3. Model parameters of the virtual robot arm.

ξ	Links	1	2	3	4	5	6
Mass values [kg] (without Wrist)							
ξ_1^i	$m_i, i = 1,...,6$	–	17.4	4.8	0.82	0.35	0.09
Link center of gravity (COG) [mm]							
ξ_2^i	S_{xi}	–	68	0	0	0	0
ξ_3^i	S_{yi}	–	6	-70	0	0	0
ξ_4^i	S_{zi}	–	-16	14	-19	0	32
Moments of inertia about COG [kgm^2]							
ξ_5^i	I_{xxi}	–	0.130	66.0e-3	1.8e-3	300e-6	150e-6
ξ_6^i	I_{yyi}	–	0.524	12.5e-3	1.8e-3	300e-6	150e-6
ξ_7^i	I_{zzi}	0.35	0.539	86.0e-3	1.3e-3	400e-6	40e-6
Effective motor inertia [kgm^2]							
ξ_8^i	J_{mi}	0.784	2.305	0.576	0.1057	0.0946	0.1074
Kinematic constants							
ξ_9^i	α_{i-1}[deg.]	0	-90	0	90	-90	90
ξ_{10}^i	a_{i-1}[m]	0	0	0.4318	-0.0203	0	0
ξ_{11}^i	d_i[m]	0	0.2435	-0.0934	0.4331	0	0
Viscous friction coefficients [Nmsec/rad]							
ξ_{12}^i	$\delta_i^-, \dot{q}_i < 0$	3.45	8.53	3.02	–	–	–
	$\delta_i^+, \dot{q}_i > 0$	4.94	7.67	3.27	–	–	–
Coulomb friction coefficients [Nm]							
ξ_{13}^i	$f_i^-, \dot{q}_i < 0$	8.26	11.34	5.57	–	–	–
	$\delta_i^+, \dot{q}_i > 0$	8.43	12.77	5.93	–	–	–

The maximal error of the iterative learning procedure is given by:

$$e^{\max} = \max_l(e_l^{\max}), \quad l = 0,1,...,N \tag{32}$$

where

$$e_l^{\max} = \max_t \|\mathbf{q}_l(t) - \mathbf{q}_d(t)\|, \quad t \in [0,T]. \tag{33}$$

In fact, there are great differences between values of ξ and $\hat{\xi}$ reported in Tab. 1 and Tab. 2, respectively. Consequently a significant maximal initial tracking error $e_0^{\max}$ is expected. Therefore, solving the nonlinear differential equation (1), for $l = 0$ $K_v = -6$ and $K_p =$

Table 4. Model parameter estimates of the virtual robot arm.

ξ	Links	1	2	3	4	5	6
Mass values [kg] (without Wrist)							
ξ_1^i	m_i, $i=1,...,6$	–	22.4	5	1.2	0.62	0.16
Link center of gravity (COG) [mm]							
ξ_2^i	S_{xi}	–	103	20	0	0	0
ξ_3^i	S_{yi}	–	5	-4	-3	-1	0
ξ_4^i	S_{zi}	–	-40	14	-86	-10	3
Moments of inertia about COG [kgm^2]							
ξ_5^i	I_{xxi}	–	0.403	74.8e-3	5.32e-3	487e-6	123e-6
ξ_6^i	I_{yyi}	–	0.969	7.3e-3	5.20e-3	482e-6	123e-6
ξ_7^i	I_{zzi}	0.177	0.965	75.6e-3	3.37e-3	572e-6	58e-6
Effective motor inertia [kgm^2]							
ξ_8^i	J_{mi}	0.776	2.34	0.5823	0.1057	0.0946	0.1074
Kinematic constants							
ξ_9^i	α_{i-1}[deg.]	0	-90	0	90	-90	90
ξ_{10}^i	a_{i-1}[m]	0	0	0.4318	-0.0203	0	0
ξ_{11}^i	d_i[m]	0	0.2435	-0.0934	0.4331	0	0
Viscous friction coefficients [Nmsec/rad]							
ξ_{12}^i	δ_i^-, $\dot{q}_i<0$	3.85	8.89	5.31	–	–	–
	δ_i^+, $\dot{q}_i>0$	3.20	11.7	2.91	–	–	–
Coulomb friction coefficients [Nm]							
ξ_{13}^i	f_i^-, $\dot{q}_i<0$	6.74	13.0	5.87	–	–	–
	δ_i^+, $\dot{q}_i>0$	7.24	14.7	4.19	–	–	–
Torque limits [Nm]							
ξ_{14}^i	$\hat{U}_i^{\max}$	100	180	90	25	25	25

-3, with $\mathbf{u}_0(t)\equiv 0$, $\mathbf{u}_c \equiv \mathbf{u}_c^{*,t}(\mathbf{q}_0,t,\hat{\xi})$ in Eq. (3), for sampling interval $t^s=0.1$[sec], and with initial conditions $\mathbf{q}_1(0)=0$, and $\dot{\mathbf{q}}_1(0)=0$ results in trajectories $\mathbf{q}_0(t)$, $(q_0^i(t))$, which are depicted in Fig. 4 together with the desired trajectories $(q_d^i(t))$.

Simulation results for the first iteration, shown in Fig. 4(a), reveal significant initial tracking errors of the second and third joints. It has to be mentioned that the on-line computation time of the feedback control (computed torque calculated by Matlab software) is from 0.0620 sec. to 0.0940 sec. and, consequently, the sampling interval of

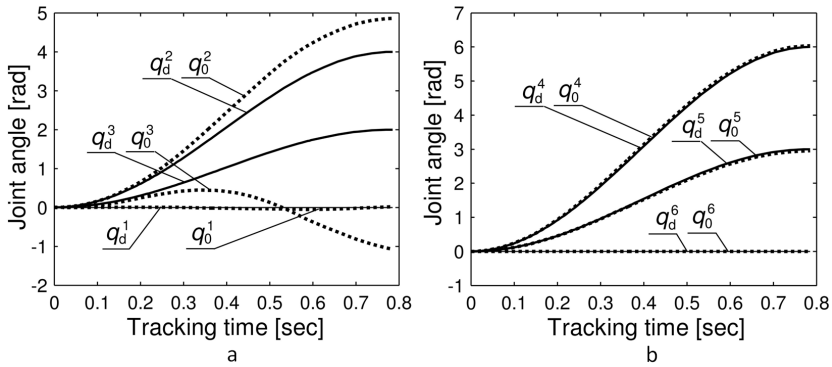

Figure 4. The initial and desired trajectories, (a) q_0^i, q_d^i, $i = 1,2,3$; (b) q_0^i, q_d^i, $i = 4,5,6$.

0.1 sec. is adequate for simulation. The time of the offline computation (update) of the feedforward control is approximately 30 sec., depending on the solution of the dynamic equations, and in real implementation this calculation time could be reduced by use of optimal spline approximation and powerfull computer system. The initial tracking error $e_0^{\max}$ given by Eq. (33) for $l = 1$ arises not only due to parameter uncertainties but also due to the large sampling interval $t^s = 0.1$[sec]. For example, $e_0^{\max} = 3.1944$[rad] for $t^s = 0.1$[sec] and $e_0^{\max} = 2.8745$[rad] for $t^s = 0.0$[sec].

The calculation of the maximal tracking errors $e_l^{\max}$ for $l = 0,1...20$ by solving the nonlinear differential equation (31) ($K_v = -6$, $K_p = -3$, $L_v = 0$, $L_p = 0$, $\mathbf{u}_0(t) \equiv 0$, $t^s = 0.1$[sec], $\mathbf{q}_l(0) = 0$, $\dot{\mathbf{q}}_l(0) = 0$) reveals the convergence behavior and the convergence rate of the proposed NILC with SD feedback. The profile of $e_i^{\max}$ versus iteration number is depicted (continuous line) in Fig. 5.

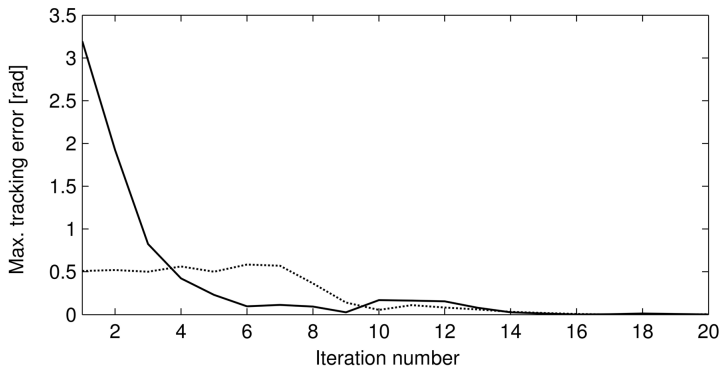

Figure 5. $e_i^{\max}$ obtained by the standard (cont. line) and bounded-error (dotted line) algorithms.

Referring to Fig. 5 one can see a fast and monotonic convergence of the iterative procedure and obviously in this case the maximal learning error $e^{\max}$ given by Eq. (32)

equals to the initial tracking error $e_0^{\max}$. But a problem for the practical application of the considered NILC arises because of the large initial error $e_0^{\max}$ and this problem can be solved by using the 'Bounded-error algorithm' for NILC presented in [10].

The profile of $e_l^{\max}$ obtained by the 'Bounded-error algorithm' (0.5[rad] error norm bound) is shown (dotted line) in Fig. 5.

In order to illustrate how the feedforward control term $\mathbf{u}_l(t)$, $t \in [0, 0.25\pi]$ compensates for the uncertainties of the sampled data feedback control term $\mathbf{u}_c^{*,t}$ we investigate by simulation the control input at the final 20th iteration which results in the profiles of $\mathbf{u}_c^{*,t}$, $\mathbf{u}_{20}$ and $\mathbf{u}$ shown in Fig. 6.

The graphs in Fig. 6(a), Fig. 6(b) and Fig. 6(c) show the feedback $(u_c^i, \mathbf{u}_c \equiv \mathbf{u}_c^{*,t})$, feedforward (u_{20}^i), and the resultant $(u^i = u_{20}^i + u_c^i,\ \ i = 1,2,3)$ control inputs for the first, second and third joints correspondingly while the Fig. 6(d), Fig. 6(e), and Fig. 6(f) illustrate the same control terms but for the fourth, fifth, and sixth joints of the robot arm.

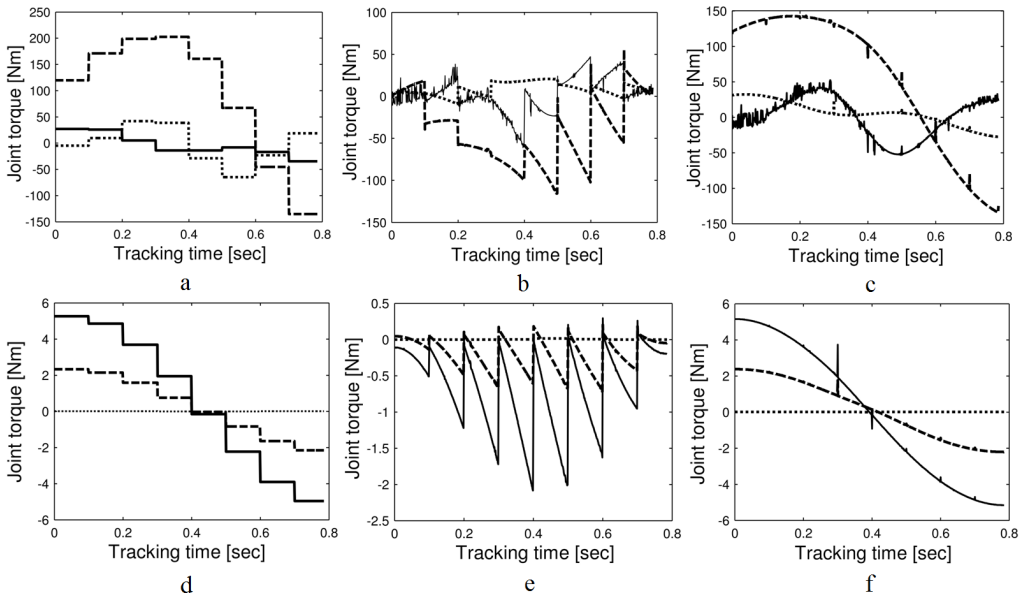

Figure 6. Feedback u_c^i: (a) $i = 1,2,3$, (d) $i = 4,5,6$; Feedforward u_{20}^i: (b) $i = 1,2,3$, (e) $i = 4,5,6$; $u^i = u_{20}^i + u_c^i$: (c) $i = 1,2,3$, (f) $i = 4,5,6$; Cont. line: $i = 1,4$; Dashed line: $i = 2,5$; Dotted line: $i = 3,6$.

Finally, the value-adding process of the continuous piecewise-constant feedback control (dotted line) and the piecewise feedforward control (dashed line) that results in the continuous control input (continuous line) of the second joint is schematically represented in Fig. 7.

The simulation result shows that the piecewise continuous feedforward control compensates for inaccuracies (instability) that arise from the piecewise-constant feedback with sampling interval 0.1 sec. This sampling interval is relatively long and makes possi-

ble real-time implementation (real-time computation) of complex dynamics-based feedback control taking into account properties of modern CPUs.

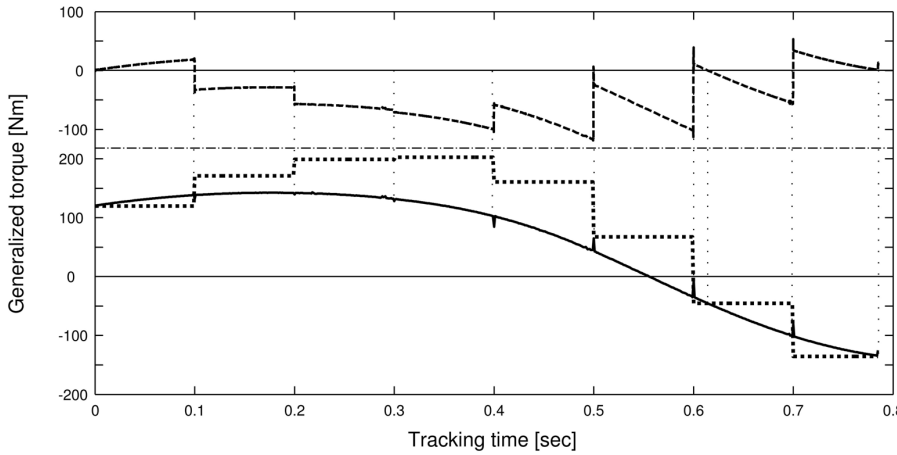

Figure 7. Feedback u_c^2 (dotted line), feedforward u_{20}^2 (dashed line) and $u^2 = u_{20}^2 + u_c^2$ (cont. line).

5. Conclusions

The continuous nonlinear iterative learning control with sampled-data feedback proposed in this paper for continuous nonlinear multiple-input multiple-output time varying systems, such as robotic manipulators, consists of two controllers (see Eq. (31)): a continuous time learning controller (see Eq. (2)) and a sampled-data (SD) feedback controller (see Eq. (3)). An off-line ILC scheme with SD feedback is presented in Fig. 3. The SD feedback is required for feedback controllers based on complicated dynamic models, for instance, dynamic models of 6 or 7 DOF robotic manipulators (see Eq. (31)). In this case, the nonlinear model based feedback control requires a lot of on-line calculations that cause a time delay and the corresponding sampling interval which should not be neglected, while the learning controller requires off-line calculations and therefore, the nonlinear model-based feedforward control can be assumed as a continuous one.

We came to the following conclusions for the proposed NILC with SD feedback for robotic manipulators:

- The robustness and convergence of the proposed NILC with SD feedback is proven (by Theorem 2) with respect to the time-weighted norm (λ norm) of the control input error.

- The sufficient condition for robustness and convergence of the proposed NILC with SD feedback is the same as the corresponding condition of a standard NILC

with a continuous feedback controller attached implying that the convergence does not depend on the sampling interval, as it is the case for other types of Sampled-data ILC (Fig 2. (a)) and Multirate ILC (Fig 2. (b)) controllers.

- The proposed NILC with SD feedback for PUMA560 robotic manipulator is robust and convergent.
- The analysis of the iterative learning control simulations on the PUMA560 robot reveals that at the final iteration the piecewise feedforward control term successfully compensates for the uncertainties of the continuous piecewise-constant feedback control term so that the sum of both terms is a continuous control input.
- The proposed solution to the instability problem in the Sampled-Data feedback is the main contribution of this paper to the ILC implementation in practice.

References

[1] A.M. PERTEW, H.J. MARQUEZ and Q. ZHAO: A direct sampled-data design approach for robot stabilization.*Proc. of the 2008 American Control Conference*, Seattle, Washington, (2008), 369-374.

[2] T. OOMEN, J. VAN DE WIJDEVEN and Q. ZHAO; Suppressing intersample behavior in iterative learning control. *Automatica* **45** (2009), 981-988.

[3] Y.-J. PAN, H.J. MARQUEZ and T. CHEN: Sampled-data iterative learning control for a class of nonlinear networked control systems. *Proc. of the 2006 American Control Conference*, Minneapolis, Minnesota, (2006), 3494-3499.

[4] T.-W. MA and H. YANG: Sampled data feedback-feedforward control of structures with time delays. *J. of Structural Engineering*, **132**(7), (2006), 1129-1138.

[5] S. ARIMOTO, S. KAWAMURA and F. MIYAZAKI: Bettering operation of dynamic systems by learning: A new control theory for servomechanism of mechatronics systems. *Proc. 23rd Conf. on Decision and Control*, Las Vegas, NV, (1984), 1064-1068.

[6] H.-S. AHN, K. MOORE and Y. CHEN: Iterative Learning Control Robustness and Monotonic Convergence for Interval Systems. Springer-Verlag London Limited, London, 2007.

[7] J.-X. XU and Y. TAN: Linear and Nonlinear Iterative Learning Control, Lecture Notes in Control and Information Sciences. Springer, New York, 2003.

[8] H.-S. AHN and D. A. BRISTOW: Special Issue on 'Iterative Learning Control', *Asian J. of Control*, **13**(1), (2011), 1-2.

[9] K. DELCHEV and E. ZAHARIEV: Computer simulation based synthesis of learning control law of robots. *Mechanics Based Design of Structures and Machines*, **36**(3), (2008), 225-248.

[10] K. DELCHEV: Iterative learning control for nonlinear systems: A bounded-error algorithm. *Asian J. of Control*, **15**(2), (2013), 453-460.

[11] B. ZHANG, D. WANG, Y. WANG, Y. YE and K. ZHOU: Comparison studies on anti-aliasing/anti-imaging filtering and signal extension in multi-rate ILC. *Proc. 17th World Congress of The International Federation of Automatic Control*, Seoul, (2008), 12468-12473.

[12] D. VASSILEVA, G. BOIADJIEV, H. KAWASAKI and T. MOURI: Force compensating trajectories for redundant robots: Experimental results. *J. of Robotics and Mechatronics*, **21**(1), (2009), 104-112.

[13] V. KOZLOV, V. MAKARYCHEV, A. TIMOFEEV and E. YUREVICH: Dynamics of Robot Control, Nauka, Moscow, 1984, (in Russian).

[14] J. ZHANG: Advanced Pulse Width Modulation Controller ICs for Buck DC-DC Converters. Ph.D. Thesis, University of California, Berkeley, 2006.

[15] R.W. LONGMAN: Iterative learning control and repetitive control for engineering practice. *Int. J. of Control*, **73**(10), (2000), 930-954.

[16] D. HEINZINGER, B. FENWICK, B. PADEN and F. MIYAZAKI: Robust learning control. *Proc. 28th Conf. on Decision and Control*, Tampa, FL, (1989), 436-440.

[17] D. HEINZINGER, B. FENWICK, B. PADEN and F. MIYAZAKI: Stability of learning control with disturbances and uncertain initial conditions. *IEEE Trans. on Automatic Control*, **37**(1), (1992), 110-114.

[18] R. JAMES and G. JAMES: Mathematics Dictionary. 5th ed., Chapman & Hall, New York, 1992.

[19] B. ARMSTRONG, O. KHATIB and J. BURDICK: The explicit dynamic model and inertial parameters of the PUMA 560 arm. *Proc. IEEE Int. Conf. Robotics and Automation*, San Francisco, USA, **1** (1986), 510-518.

[20] P. CORKE and B. ARMSTRONG-HELOUVRY: A search for consensus among model parameters reported for the PUMA 560 robot. *Proc. IEEE Int. Conf. Robotics and Automation*, San Diego, USA, **1** (1994), 1608-1613.

[21] T. TARN, K. BEJCZY, S. HAN and X. YUN: Inertia parameters of Puma 560 robot arm. Tech. Rep. SSM-RL-85-01, Washington University, St. Louis, MO, 1985.

Appendix 1

Lemma 5 *If $h(t_k) \equiv h^k$ is a discrete form of $h(t)$, $t \in [0,T]$, $\{t_k : t_k = kt^s\}_{k=0}^{K} \subset [0,T]$, $K = \lfloor T/t^s \rfloor$, t^s is the sampling interval and $h^{*,t} \equiv h^*(h^k,t)$ is the corresponding continuous piecewise-constant function on $[0,T]$, then $\|h^{*,t}\|_\lambda \leqslant \|h(t)\|_\lambda$.*

Proof The λ norm of $h(t)$, $t \in [0,T]$ is defined by

$$\|h(t)\|_\lambda \equiv \sup_{t\in[0,T]} e^{-\lambda t} \|h(t)\|. \tag{A.1}$$

For continuous piecewise-constant functions it has to be mentioned that $\left\|h^*(h^k,t)\right\| = \left\|h^k\right\|$, $\forall t \in [t_k, t_{k+1}) \cup [t_K, T]$, $t_0 = 0$, $k = 0,1,...,K-1$, $K = \lfloor T/t^s \rfloor$.

Using $\left\|h^*(h^k,t)\right\| = \left\|h^k\right\|$ for the right-hand side of the definition (A.1) it follows:

$$\begin{aligned}
&\sup_{t\in[t_k,t_{k+1})} e^{-\lambda t} \left\|h^*(h^k,t)\right\| = \left\|h^k\right\| \sup_{t\in[t_k,t_{k+1})} e^{-\lambda t} \\
&\left\|h^k\right\| \sup_{t\in[t_k,t_{k+1})} e^{-\lambda t} = e^{-\lambda t_k} \left\|h^k\right\|, k = 0,1...K-1; \\
&\sup_{t\in[t_K,T]} e^{-\lambda t} \left\|h^*(h^K,t)\right\| = e^{-\lambda t_K} \left\|h^K\right\|.
\end{aligned} \tag{A.2}$$

On the other hand for $t \in [0,T]$

$$e^{-\lambda t} \left\|h^*(h^k,t)\right\| = \bigcup_{k=0}^{K-1} \left\{ e^{-\lambda t} \left\|h^*(h^k,t)\right\|, t \in [t_k,t_{k+1}) \right\} \cup \left\{ e^{-\lambda t} \left\|h^*(h^K,t)\right\|, t \in [t_K,T] \right\}. \tag{A.3}$$

Thus, from Eq. (A.2) and Eq. (A.3) it follows:

$$\sup_{t\in[0,T]} e^{-\lambda t} \left\|h^*(h^k,t)\right\| = \max_k e^{-\lambda t_k} \left\|h^k\right\|, k = 0,1,...,K \tag{A.4}$$

but $\left\|h^k\right\| \equiv \|h(t_k)\|$, $k = 0,1,...,K$, $t \in [0,T]$ and

$$\max_k e^{-\lambda t_k} \|h(t_k)\| \leqslant \sup_{t\in[0,T]} e^{-\lambda t} \|h(t)\|. \tag{A.5}$$

From Eq. (A.4) and inequality (A.5) we have

$$\sup_{t\in[0,T]} e^{-\lambda t} \left\|h^*(h^k,t)\right\| \leqslant \sup_{t\in[0,T]} e^{-\lambda t} \|h(t)\| \tag{A.6}$$

and using the definition (A.1), we obtain from inequality (A.6) that $\|h^{*,t}\|_\lambda \leqslant \|h(t)\|_\lambda$.